Surgical Neurology International

OPEN ACCESS

For entire Editorial Board visit : http://www.surgicalneurologyint.com

Editor-in-Chief: **James I. Ausman,** MD, PhD University of California, Los Angeles, CA, USA

Original Article

Reproducibility of quantitative fiber tracking measurements in diffusion tensor imaging of frontal lobe tracts: A protocol based on the fiber dissection technique

Leandro I. Dini[1,2], Leonardo M. Vedolin[3], Debora Bertholdo[3], Rafael D. Grando[3], Alessandro Mazzola[3], Simone A. Dini[2], Gustavo R. Isolan[2], Jaderson C. da Costa[4], Alvaro Campero[5]

[1]Neurosurgery, Grupo Hospitalar Conceição (GHC), Porto Alegre, RS, Brazil; [2]Neurosurgery, Fundação Hospital Centenário, São Leopoldo, RS, Brazil; [3]Neuroradiology, Hospital Moinhos de Vento (HMV), Porto Alegre, RS, Brazil; [4]Neurology, Pontifícia Universidade Católica do Rio Grande do Sul (PUCRS), Porto Alegre, RS, Brazil; [5]Neurosurgery, Hospital Padilla, Tucumán, Argentina

E-mail: *Leandro I. Dini - leandrodini@ig.com.br; Leonardo M. Vedolin -leonardovedolin@hotmail.com; Debora Bertholdo - debora.berth@onda.com.br; Rafael D. Grando - rdgrando@hotmail.com; Alessandro Mazzola - mazzola.ci@hmv.org.br; Simone A. Dini - dini.simone@yahoo.com; Gustavo R. Isolan - gisolan@yahoo.com.br; Jaderson C. da Costa - jcc@pucrs.br; Alvaro Campero - alvarocampero@yahoo.com.ar
*Corresponding author

Received: 16 December 12 Accepted: 08 March 13 Published: 12 April 13

This article may be cited as:
Dini LI, Vedolin LM, Bertholdo D, Grando RD, Mazzola A, Dini SA, *et al.* Reproducibility of quantitative fiber tracking measurements in diffusion tensor imaging of frontal lobe tracts: A protocol based on the fiber dissection technique. Surg Neurol Int 2013;4:51.
Available FREE in open access from: http://www.surgicalneurologyint.com/text.asp?2013/4/1/51/110508

Abstract

Background: Diffusion tensor imaging (DTI)-based tractography is a noninvasive *in vivo* method for tracing white matter bundles. This raises possibilities for qualitative and quantitative assessment of the structural organization of tracts. Nevertheless, questions remain about neuroanatomical accuracy, reproducibility for clinical purposes, and accessibility of the best method for broader application. The aim of this study was to combine the fiber dissection technique and tractography to provide more pertinent insight into brain anatomy and, as a result, to test a protocol for reconstruction of six major frontal lobe tracts.

Methods: A combination of fiber dissection of formalin-fixed brain tissue after freezing (Klingler's technique) and virtual dissection (tractography) was used to develop a protocol to reconstruct major frontal tracts. Apparent diffusion coefficient (ADC), fractional anisotropy (FA), number of voxels (NVO), volume (VOL), number (NTR), and length (LEN) of tracts were evaluated to assess intra- and interobserver reproducibility. Statistical reliability was evaluated using intraclass correlation coefficients (ICCs) and the Pearson association coefficient (r).

Results: The virtual dissection obtained by tractography seemed to reproduce the anatomic knowledge of the white matter tracts obtained through the classic method. In reliability study, most ICC and r values corresponded at least to large correlation. The magnitude of correlation was *very high* (ICC 0.7-0.9) or *almost perfect* (ICC 0.9-1.0) for the FA and ADC measures of every tract studied.

Conclusion: The DTI protocol proposed herein provided a reliable method for analysis of reconstructed frontal lobe tracts, especially for the FA and ADC variables.

Key Words: Anatomy, diffusion tensor imaging, frontal lobe

Access this article online

Website: www.surgicalneurologyint.com

DOI: 10.4103/2152-7806.110508

Quick Response Code:

INTRODUCTION

Tractography based on diffusion tensor imaging (DTI) has enabled exploration of the white matter in a unique way. Through mathematical analysis of the diffusion properties of water molecules in the parenchyma, white matter bundles can be recreated in three-dimensional (3D). This has made actual virtual dissection of the human brain and structural quantitative analysis of the brain a possibility, which allows the integrity of selected tracts to be estimated.

Despite the existence of many different applications for tractography in the neurosciences, no method for identifying bundles is uniform across different research projects.[21] Furthermore, even tractography atlases are not unanimous [Table 1][4,30,29,7,6,20], in particular with relation to three aspects: (1) the presence of comparisons between magnetic resonance imaging (MRI)-recreated bundles and anatomic dissections, using a specific method;[27] (2) the presence of reproducibility studies; and (3) the degree of accessibility for general radiologists. The ideal method is still being sought; that is, one which does not involve manual region of interest (ROI) selection, is not time consuming, is accessible for both clinical and research applications, and identifies tracts in a manner that is automatic, reproducible and faithful to anatomy, even when structural damage is present.

Currently, anatomical knowledge is still indispensable, whether to conceive an atlas or to interpret results. Therefore, the traditional fundamentals of anatomy, acquired with the classical fiber dissection technique, have paradoxically become even more relevant for critical judgment of tractography findings. In this study, the fiber dissection technique was used to provide anatomical knowledge to serve as the foundation for a DTI-based virtual dissection and for the development of simplified protocols for major frontal lobe tracts. The reproducibility of these protocols was then tested by raters who had no previous tractography experience (intra- and interobserver reliability).

MATERIALS AND METHODS

Anatomic study

Fiber dissection technique (Klingler's technique)

The fiber dissection technique involves layered dissection of the cerebral white matter to reveal the internal anatomic organization of the parenchyma. As an improvement to this method, Klingler *et al*. demonstrated that, when specimens are frozen, formalin crystals are formed. As they expand, these crystals separate the fibers, making dissection easier.[27] This method has been revived by contemporary authors and once more presented as the best way of learning about the 3D anatomy of the brain.[8,27] In this study, two adult human brain specimens were fixed in a 10% formalin solution for at least 2 months. The specimens were washed and then frozen at a temperature of −15°C for 1 week. After this period, they were immersed in water until thawed and dissection was begun with the aid of a surgical microscope (6x and 40x magnification). The anatomical specimens were stored immersed in 5% formalin solution between dissection sessions.

Dissections were basically performed using wooden spatulas, starting from the lateral surface. As the cortex is scraped away with the spatula, a difference can be felt between the consistency of the cortex and underlying white matter; the former is porous and friable, whereas the latter is firm and can be peeled away in layers. Removal of the cortex and successive layers of fibers progressively reveals the deeper anatomy. We followed a clear and objective guide to the procedure written by Ture *et al*.,[27] covering the stages of dissection and intended to revive use of this technique by those studying the subject.

The most reliable 3D anatomical findings related to the tracts were compiled and stored to be used in the manual selection of the ROIs during the subsequent work of tract processing on the workstation. In the different regions we selected and investigated, the massive presence of the fibers of each target tract was required. Therefore, the combination of multiple

Table 1: Studies on tractography including intra- and interobserver agreement tests

Authors	Anatomic study	Statistical analysis	Variables	Intraobserver	Interobserver
Catani *et al.*[3]	No	r	FA, VOL, LEN, NTR	No	10 observers vs. 1 observer
Wakana *et al.*[27]	No	kappa, CV	FA, PIXELS	1 observer	3 observers**
Verhoeven *et al.*[29]	No	kappa	PIXELS	3 observers	3 observers
Danielian *et al.*[6]	No	ICC, kappa, CV	MD, FA, AD, TD, PIXELS	2 observers	2 observers
Ciccarelli *et al.*[5]	No	CV	VOL, FA	1 observer	2 observers
Malykhin *et al.*[20]	No	ICC, CV	VOL, ADC, FA	1 observer	2 observers
Bonekamp *et al.*[1]	No	ICC, CV	ADC, FA	1 observer	4 observers
This study	Yes	ICC, r	FA, VOL, NTR, LEN, ADC, NVO	2 observers	2 observers*

*Without previous experience with this method. ADC: Apparent diffusion coefficient; CV: Coefficient of variance; r: Pearson association coefficient; ICC: Intraclass correlation coefficients; FA: Fractional anisotropy; VOL: Volume; LEN: Length of tracts; NTR: Number of tracts; MD: Mean diffusivity; AD: Axial diffusivity; TD: Transverse diffusivity; NVO: Number of voxels

ROIs with these fibers allowed improving anatomical sensitivity and specificity at a later phase.

Those fibers present in two of the ROIs selected based on the anatomical study and the ones showing on the tractography the same morphology found in the dissections will be considered as belonging to the tract being investigated.

Virtual dissection technique (DTI-based Tractography)

Subjects and imaging

DTI-MR images were obtained from our institution's existing data set, including 15 normal subjects (10 male and 5 female). Mean age was 35 ± 8.6 years. All measurements were performed for both hemispheres. Approval was obtained from the local institutional review board.

All scans were performed on a Siemens 1.5T Avanto 76 × 18 MRI system (Siemens, Erlangen, Germany) using a 12-channel head matrix coil and a maximum gradient amplitude of 45 mT/m. The protocol was optimized for 40-axial-slice DTI acquisition with 12 directions, two b-values (0 and 1000 s/mm^2), four averages, a repetition time of 6500 ms, an echo time of 96 ms and using a parallel acquisition technique with a factor of two. The field of view was 240 mm, matrix size was 192 × 192, resulting in voxel size of 1.25 × 1.25 × 2.5 mm^3. No interpolation was used. Data were exported to a multipurpose workstation, and the Neuro3D software integrated with an offline-processing Diffusion Tensor and MR Diffusion Tracts (Siemens, Erlangen, Germany) was used to process tracts. This software package provides six quantitative measures of the set of voxels for each reconstructed structure, using the selected ROIs and parameters.

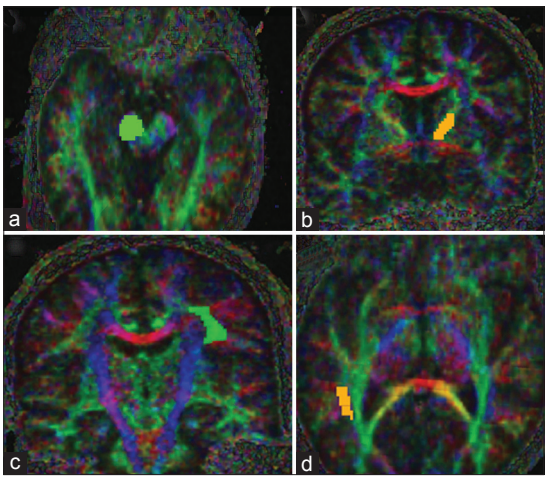

Figure 1: Locations of the ROIs for frontal lobe tracts on the directional maps (a-d). A = ROI 1 is located on the cerebral peduncle base for FP. B= ROI 2 (orange) for FP. C= ROI 1(green) for ARC; it is the one-ROI for SLF. D= ROI 2 (orange) for ARC. ARC= arcuate fasciculus; FP= frontopontine fibers; ROI= region of interest; SLF= superior longitudinal fasciculus

Reconstruction protocol

The authors attempted to reconstruct the same tracts and structures identified in the prior anatomic study, seeking analogy between the virtual anatomy and the dissections. In addition to using existing atlases as a reference, the authors used the 3D knowledge acquired from dissections as a basis for this stage of the study. Whenever the selected ROIs did not allow the characteristic morphology and path of the tract to be reproduced, thresholds, landmarks, and/or ROI tracing were corrected. In other words, if a bundle reproduced from ROIs was not consistent with the conformation expected on the basis of anatomic studies, the authors attempted to optimize the outline of ROIs or the thresholds for angle, fractional anisotropy (FA), and Step Length. Only then were landmarks defined as part of the protocol.

A multi-ROI approach was chosen to reconstruct several tracts of interest, exploiting existing anatomical knowledge of tract pathways. The combination of the selected ROIs and parameters enabled an adequate final reconstruction. Exclusion ROIs were not employed. Landmarks were defined on color-coded maps [Figures 1 and 2].

In this study, we focused specifically on testing reproducibility with six frontal lobe white matter bundles. A reconstruction protocol was created for each bundle, containing a pictorial review of the reconstruction [Figures 3-5] together with the information described below.

Superior longitudinal fasciculus

The superior longitudinal fasciculus (SLF) is a massive bundle of association fibers that forms a wide arc around

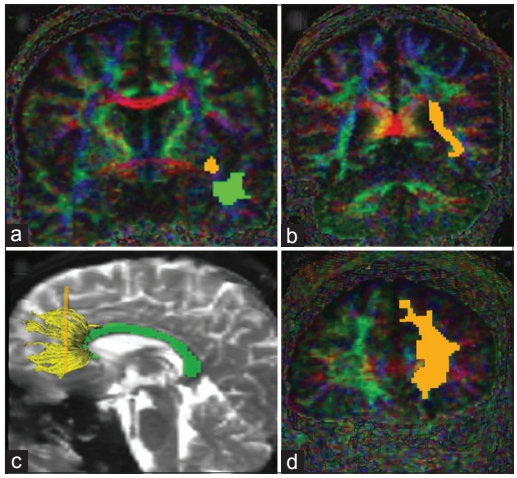

Figure 2: Locations of the ROIs for frontal lobe tracts on the directional maps (a-d) and tractography of the GCC (yellow) on b0, an acquisition with similar T2-weighted images. A = ROI 1 (green) and ROI 2 (orange) for UNC. B= ROI 2 (orange) for IFO; ROI 1 is the same as ROI 2 for UNC; C and D= ROI 1 (green) and ROI 2 (orange) for GCC. ARC= arcuate fasciculus; GCC= genu of corpus callosum; IFO= inferior fronto occipital fasciculus; ROI= region of interest; UNC= uncinate fasciculus

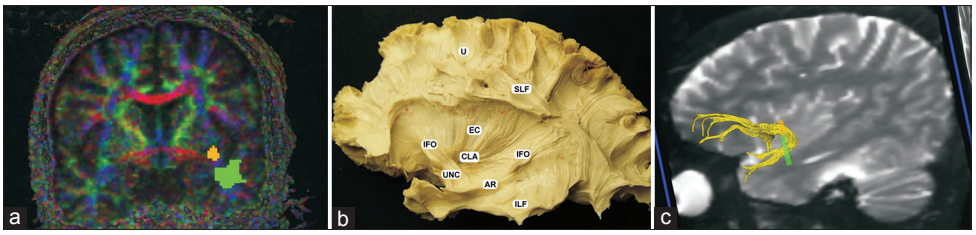

Figure 3: An example protocol for tract reconstruction as used in this study (UNC, in this example). Each protocol was based on theoretical information (see "Methods" section), an image showing the selected ROIs on the color-coded map (a), an image of the tract as determined by the fiber dissection technique (b), and an image of the tract obtained by DTI-based tractography (c). U = U fibers; UNC = uncinate fasciculus; CLA = claustrum; SLF = superior longitudinal fasciculus; EC = external capsule; IFO = inferior fronto-occipital fasciculus; AR = arcuate fasciculus; ILF = inferior longitudinal fasciculus

the superior border of the insula, connecting the cortices of the frontal, parietal, temporal, and occipital lobes. The "C"-shaped SLF is the widest association bundle [Figure 5].

A single ROI was placed on the coronal slice on which the cerebral peduncle and basilar part of the pons (transverse fibers are shown in red) could be seen clearly. The ROI drawing includes the green area lateral to the corona radiata (shown in blue), above the superior sulci of the insula, deeply sited in the inferior frontal gyrus [Figure 2]. Thresholds used were angle 30°, FA 0.2, and Step Length 0.68.

Uncinate fasciculus

"Uncinate," from the Latin *uncus*, means "hook-shaped." This structure curves around the lateral sulcus to connect the inferior and orbital frontal gyri to the anterior temporal lobe. The anterior portion of this relatively short tract is located inferior and medial to the fronto-occipital fasciculus. At its middle portion, the uncinate fasciculus (UNC) becomes adjacent to the fronto-occipital fasciculus, before curving inferiorly and laterally toward the temporal pole and the middle and superior temporal gyri [Figures 3 and 4].

ROIs were placed on the coronal slice on which the anterior commissure and amygdala (best identified on b0) could be best seen in full profile. ROI 1 included the green area lateral to the amygdala, inside the temporal lobe. ROI 2 was located in the green area above the amygdala and medial to the insular cortex, inside the frontal lobe [Figure 1]. Thresholds used were angle 40°, FA 0.2, and Step Length 0.9.

Frontopontine fibers

The internal capsule is a wide, compact bundle of fibers that serves as a corridor of sorts for most projection fibers arising from the brain or leading into it. The anterior limb of the internal capsule is located between the head of the caudate nucleus and the rostral aspect of the lentiform nucleus, and contains the frontopontine fibers (FP) arranged anteroposteriorly [Figure 5].

ROI 1 was placed on the axial slice corresponding to the base of the cerebral peduncle, at the same level as the

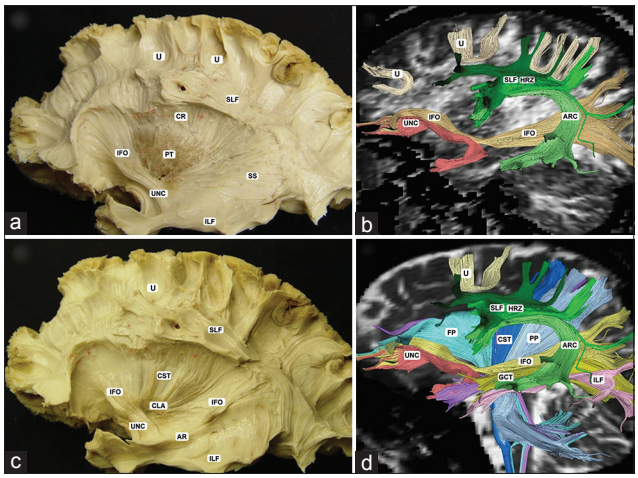

Figure 4: Comparison between anatomic dissections using the fiber dissection technique and tractography. Qualitative analysis of tract reconstruction using DTI; b0 images of the contralateral hemisphere are used as background for spatial orientation. (a and c) gross dissection, lateral view. (b and d) tractographies. ARC = arcuate fasciculus; CLA = claustrum; CR = corona radiata; HRZ = horizontal segment; IFO = inferior fronto-occipital fasciculus; ILF = inferior longitudinal fasciculus; PT = putamen; AR = auditory radiation; SLF = superior longitudinal fasciculus; SS = sagittal stratum; UNC = uncinate fasciculus; U = U fibers; GCT = geniculocalcarine tract; CST = corticospinal tract; PP = parietopontine fibers; FP = frontopontine fibers

superior colliculus (best seen on b0). ROI 2 was the green area, delimited above at the level of half of the caudate head nucleus on a coronal slice, including the boundary with the lenticular nucleus [Figure 2]. Marking on the medial limits of this area should be avoided so as not to include thalamic radiation fibers.

The thresholds used were angle 25°, FA 0.2, and Step Length 0.68.

Inferior fronto-occipital fasciculus

This fasciculus connects the frontal and occipital lobes, but in a more inferior and external location. It extends deep into the insula and is closely related to the claustrum in an inferolateral direction. Posteriorly, the inferior fronto-occipital fasciculus (IFO) follows a course parallel to the fibers of the anterior commissure, UNC, and geniculocalcarine tract to contribute to the

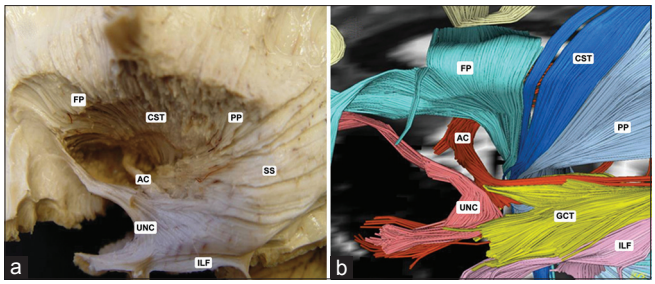

Figure 5: Comparison between anatomic dissections using the fiber dissection technique and tractography. Qualitative analysis of tract reconstruction using DTI; b0 images of the contralateral hemisphere are used as background for spatial orientation. (a) gross dissection, lateral view; U fibers, SLF, IFO, the nucleus of CL, PT and GP, as well as part of UNC were removed. (b) tractographies. AC is divided into anterior and posterior arm. Whereas, in dissection, it is not possible to identify clear borders between parallel structures and the exposure of a bundle that may require the destruction of a more superficial bundle, tractography enables overlaying of segmented structures using different colors to provide a new view of the relationship between different bundles. AC = anterior commissure; ILF = inferior longitudinal fasciculus; FP = frontopontine fibers; IFO = inferior fronto-occipital fasciculus; PP = parietopontine fibers; PT = putamen; SLF = superior longitudinal fasciculus; SS = sagittal stratum; CST = corticospinal tract; GCT = geniculocalcarine tract; UNC = uncinate fasciculus

formation of the sagittal stratum, a broad and complex fiber bundle that connects the occipital lobe to the rest of the brain [Figure 5].

ROI 1 for the IFO is the same as ROI 2 for the UNC. The second IFO ROI was placed on the green area lateral to the atrium of the lateral ventricle (above) and posterior thalamus (below), on the coronal slice showing corpus callosum splenium, atrium and posterior thalamus [Figure 1]. The thresholds used were angle 23°, FA 0.2, and Step Length 0.68.

Genu of the corpus callosum

The genu of the corpus callosum (GCC) is the most voluminous white matter bundle and connects corresponding cortical areas across the two hemispheres, except for the temporal poles, which are connected by the anterior commissure. The fibers of the body of the corpus callosum are arranged transversely, whereas those of the genu curve anteriorly and posteriorly to reach the anterior and posterior poles of the hemispheres [Figure 1].

ROI 1 was placed on the most medial sagittal slice (best seen on b0) where the GCC was seen in full profile. ROI 2 was an entire green region located on the coronal slice immediately ahead of the anterior limit of ROI 1. The thresholds used were angle 20°, FA 0.2, and Step Length 0.68.

Arcuate fasciculus

A segment of the SLF that connects areas of the frontal and temporal lobes. It connects language areas in the left hemisphere [Figure 5].

ROI 1 is identical to the SLF ROI. ROI 2 was placed in the axial slice, corresponding to a thin blue region, lateral to a green area (sagittal stratum), at the level at which the atrium is best seen [Figure 2]. Thresholds used were angle 30°, FA 0.2, and Step Length 0.68.

Intraobserver and interobserver reproducibility

A selection of theoretical information and visual data were compiled on A4 sheets to produce a protocol for each bundle comprising the following: An image of the structure as dissected using the classical anatomic method; a virtual image of the bundle as obtained by tractography; an image showing the color map on which ROIs were selected; a chart providing theoretical information; and the thresholds used to obtain the bundle in question [Figure 3].

These protocols were then given to two radiologists who were unfamiliar with the method to guide them in reconstructing each bundle. Within 1 week, these observers reconstructed all of the bundles of interest for each of the 30 hemispheres, and then repeated each reconstruction 7 days later.

Six quantitative DTI tracking measurements (FA, volume [VOL], number of voxels [NVO], number [NTR], and length [LEN]) were evaluated for each of the six different tracts (arcuate fasciculus [ARC], UNC, IFO, SLF, GCC, and FP). For each observer, the results of the two reconstructions were compared in order to study intraobserver agreement, and the mean results for each observer were used to calculate interobserver agreement.

Intraobserver and interobserver reliability for fiber tracking measurements were determined using the intraclass correlation coefficient (ICC) and Pearson's correlation coefficient (r). For each variable of each reconstructed structure, the mean ICCs and mean intra- and interobserver correlation coefficients were calculated. The results were entered into a spreadsheet for comparison [Table 2]. Data were analyzed using the Statistical Package for the Social Sciences (SPSS) 11.5 software (SPSS Inc., Chicago, IL, USA). According to the criteria defined by Hopkins,[12] an ICC value of 0.0-0.1 is considered "trivial," 0.1-0.2 is "small," 0.3-0.5 is "moderate," 0.5-0.7 is "large,"0.7-0.9 is "very large," and 0.9-1 is "nearly perfect" agreement.

RESULTS

Reproducibility measurements

Table 2 lists the means for the measures of association (r) and agreement (ICC) achieved by the observers reconstructing the structures UNC, IFO, GCC, FP, ARC, and SLF. The values of r were superior or at least equivalent to the results for ICC for all of the structures and variables. The medians of the variables related to the ICC reached a very high level of agreement for the IFO, GCC, ARC, and SLF structures.

Table 2: Measures of intraobserver and interobserver association (r: Pearson's coefficient) and agreement (ICC: Intraclass correlation coefficient by agreement method) for reconstruction of the structures UNC, IFO, GCC, FP, ARC and SLF

Structure	Intraobserver 1				Intraobserver 2				Interobserver			
	r	*P*	ICC	*P*	r	*P*	ICC	*P*	r	*P*	ICC	*P*
UNC_NTR	0.79	<0.001	0.72	<0.001	0.52	0.003	0.52	0.001	0.46	0.012	0.45	0.005
UNC_NVO	0.83	<0.001	0.79	<0.001	0.53	0.003	0.52	0.001	0.67	<0.001	0.64	<0.001
UNC_VOL	0.83	<0.001	0.79	<0.001	0.53	0.003	0.52	0.001	0.67	<0.001	0.64	<0.001
UNC_LEN	0.74	<0.001	0.74	<0.001	0.60	0.001	0.60	<0.001	0.73	<0.001	0.66	<0.001
UNC_FA	0.81	<0.001	0.80	<0.001	0.85	<0.001	0.85	<0.001	0.84	<0.001	0.80	<0.001
UNC_ADC	0.79	<0.001	0.77	<0.001	0.87	<0.001	0.86	<0.001	0.81	<0.001	0.76	<0.001
Median			0.78				0.56				0.65	
IFO_NTR	0.72	<0.001	0.69	<0.001	0.79	<0.001	0.79	<0.001	0.89	<0.001	0.88	<0.001
IFO_NVO	0.74	<0.001	0.72	<0.001	0.87	<0.001	0.87	<0.001	0.91	<0.001	0.86	<0.001
IFO_VOL	0.74	<0.001	0.72	<0.001	0.77	<0.001	0.77	<0.001	0.88	<0.001	0.84	<0.001
IFO_LEN	0.78	<0.001	0.77	<0.001	0.87	<0.001	0.86	<0.001	0.85	<0.001	0.85	<0.001
IFO_FA	0.86	<0.001	0.83	<0.001	0.89	<0.001	0.83	<0.001	0.90	<0.001	0.90	<0.001
IFO_ADC	0.93	<0.001	0.93	<0.001	0.89	<0.001	0.89	<0.001	0.95	<0.001	0.95	<0.001
Median			0.74				0.84				0.87	
GCC_NTR	0.79	<0.001	0.78	<0.001	0.63	<0.001	0.62	<0.001	0.72	<0.001	0.69	<0.001
GCC_NVO	0.87	<0.001	0.87	<0.001	0.78	<0.001	0.77	<0.001	0.84	<0.001	0.81	<0.001
GCC_VOL	0.87	<0.001	0.87	<0.001	0.78	<0.001	0.77	<0.001	0.84	<0.001	0.81	<0.001
GCC_LEN	0.89	<0.001	0.89	<0.001	0.65	<0.001	0.52	0.002	0.77	<0.001	0.75	<0.001
GCC_FA	0.97	<0.001	0.97	<0.001	0.96	<0.001	0.95	<0.001	0.97	<0.001	0.97	<0.001
GCC_ADC	0.96	<0.001	0.95	<0.001	0.93	<0.001	0.93	<0.001	0.95	<0.001	0.91	<0.001
Median			0.88				0.77				0.81	
FP_NTR	0.29	0.127	0.29	0.063	0.49	0.006	0.45	0.005	0.55	0.001	0.26	0.003
FP_NVO	0.49	0.006	0.49	0.003	0.60	0.001	0.60	<0.001	0.66	<0.001	0.39	<0.001
FP_VOL	0.49	0.006	0.49	0.003	0.60	0.001	0.60	<0.001	0.66	<0.001	0.39	<0.001
FP_LEN	0.68	<0.001	0.68	<0.001	0.62	<0.001	0.58	<0.001	0.76	<0.001	0.73	<0.001
FP_FA	0.90	<0.001	0.90	<0.001	0.60	<0.001	0.60	<0.001	0.86	<0.001	0.81	<0.001
FP_ADC	0.84	<0.001	0.84	<0.001	0.88	<0.001	0.89	<0.001	0.77	<0.001	0.77	<0.001
Median			0.59				0.60				0.56	
ARC_NTR	0.55	0.002	0.56	0.001	0.91	<0.001	0.91	<0.001	0.79	<0.001	0.75	<0.001
ARC_NVO	0.63	<0.001	0.62	<0.001	0.92	<0.001	0.92	<0.001	0.84	<0.001	0.79	<0.001
ARC_VOL	0.61	<0.001	0.60	<0.001	0.92	<0.001	0.92	<0.001	0.86	<0.001	0.80	<0.001
ARC_LEN	0.13	0.512	0.00	0.497	0.86	<0.001	0.86	<0.001	0.19	0.319	0.00	0.495
ARC_FA	0.92	<0.001	0.91	<0.001	0.96	<0.001	0.96	<0.001	0.93	<0.001	0.93	<0.001
ARC_ADC	0.98	<0.001	0.98	<0.001	0.99	<0.001	0.99	<0.001	0.98	<0.001	0.98	<0.001
Median			0.61				0.92				0.79	
SLF_NTR	0.32	0.318	0.16	0.43	0.22	0.253	0.22	0.124	0.59	0.001	0.55	0.001
SLF_NVO	0.55	0.001	0.52	0.001	0.75	<0.001	0.74	<0.001	0.87	<0.001	0.83	<0.001
SLF_VOL	0.57	0.001	0.51	0.001	0.67	<0.001	0.65	<0.001	0.84	<0.001	0.82	<0.001
SLF_LEN	0.61	<0.001	0.49	<0.001	0.82	<0.001	0.82	<0.001	0.86	<0.001	0.86	<0.001
SLF_FA	0.88	<0.001	0.80	<0.001	0.91	<0.001	0.90	<0.001	0.93	<0.001	0.93	<0.001
SLF_ADC	0.97	<0.001	0.97	<0.001	0.98	<0.001	0.98	<0.001	0.99	<0.001	0.99	<0.001
Median			0.52				0.78				0.85	

UNC: Uncinate fasciculus; IFO: Inferior fronto-occipital fasciculus; GCC: Genu of the corpus callosum; NTR: Number of tracts; NVO: Number of voxels; VOL:Volume; LEN: Length of tracts; FA: Fractional anisotropy; ADC: Apparent diffusion coefficient; FP: Frontopontine fibers; ARC: Arcuate fasciculus; SLF: Superior longitudinal fasciculus

The magnitude of intra- and interobserver correlation was *very large* (ICC 0.7-0.9) or *almost perfect* (ICC 0.9-1.0) for the FA and apparent diffusion coefficient (ADC) measures of every tract studied. Almost all the variables for the IFO, GCC, ARC, and SLF tracts had ICCs greater than 0.7 for interobserver analyses, the exceptions being NTR of GCC and SLF and LEN of ARC. Between observers, the structures with a better than *high* level of agreement were the IFO, GCC, ARC, and SLF, specifically for FA and ADC [Table 2].

DISCUSSION

DTI-based tractography makes it possible to look at white matter bundles *in vivo* and analyze the integrity of white matter in a quantitative manner. By using this technique, researchers are able to visualize the path of least resistance to water diffusion along white matter fibers. Although tractography does not directly demonstrate fibers in the sense that injected tracers do, it is the only technique available for tracing white matter pathways in the living brain. For this reason, this technology has contributed to several areas of neuroscience. Although tractography offers impressive images and quantitative data, its limitations must be taken into account. A recurrent problem that can compromise the validity of this neuroimaging method is the occurrence of false positive and false negative results.[7,17,30] A perennial question is whether tractography is reflecting the true neuroanatomy. For example, the frontopontine fibers extend into cortical areas. In this study, these superficial projections were not identified [Figure 5], probably because of the massive projection of fibers in the transverse direction (corpus callosum). Another source of inaccuracy, which does not reside in the method *per se*, is the subjective interpretation of the examiner. For example, even when consulting complete atlases that are considered reference works on the subject,[4,26] in ignoring the fact that the anterior commissure has an anterior division and a posterior limb together with the fibers of the sagittal stratum, an operator may come to accept an incomplete reconstruction of the structure as being correct [Figure 5]. Therefore, interpretation of the results should be more precise if it is based on a solid anatomic foundation.

One of the variables involved in bundle identification that is most often debated is use of a manual ROI selection technique.[11,30] Critics of this methodology claim that the strategy requires anatomic knowledge and training and that it is excessively time-consuming, particularly if the objective is serial reconstruction of several tracts or reconstruction of tracts with more complex paths.[19,33]

In contrast, when using ROIs that are faithful to the anatomy of the tract of interest and are easily identified by the operator, small variations in the way the ROI is drawn do not appear to compromise the performance of the protocol in terms of reproducibility.[14,30] Along these methodological lines, Wakana *et al*.[30] developed protocols for reproducible identification of the principal cerebral tracts. In agreement with Wakana *et al*.,[30] the results of this study suggest that elevated reproducibility can be achieved with protocols based on manual ROI selection, as long as they provide relevant and accessible information, even when operators have no experience with the method. Nevertheless, not all tracts and variables are appropriate for simplified manual protocols, and specific testing is warranted.

The search for methods with both accuracy and reproducibility has motivated several authors to publish their techniques.[13,19,23,24,31] Atlas-based tractography, automatic ROI selection programs and analysis techniques that process pixels for the whole brain have all been proposed as means of controlling human error in ROI selection.[8,32] Nevertheless, these programs have other potential sources of variability and require detailed postprocessing. The processes involved in transformation of the images that have been thus acquired demand anatomic deformations that may be insufficient to compensate for the morphological discrepancies between different subjects.[2] It is known that small errors in spatial alignment can produce significant reorientation errors in the diffusion tensors.[28] Furthermore, these sophisticated methods require specialist intervention during image processing and very robust computer systems. It is worth noting that automatic reconstruction atlases do not have the versatility necessary to analyze tracts that were not expected to be segmented when the atlas was published, nor the ability to analyze normal structures deformed by the presence of structural damage. Irrespective of the tractography method, the reliability and interpretability of fiber tracking procedures is improved when *a priori* anatomical information is used as a guide.[10]

Over the course of the past century, several methods were developed to enable visualization of white matter tracts through a variety of histological techniques and visualization of axonal transport by means of tracer injection in animal models.[3] Despite the precise and invaluable information provided by these histological methods, they do not allow direct anatomic correlation and are not suitable for clinical studies. Kier *et al*.[18] proposed a slightly different method for locating and validating white matter bundles by obtaining MRI scans at various stages of dissection of formalin-fixed brains.

In the absence of a gold standard, the fiber dissection technique is the best method for learning the 3D anatomy of the white matter of the human brain. This technique requires an anatomic specimen prepared by freezing and simple instruments for dissection. This method, a valuable exercise that is both hands-on and intellectual, enables acquisition of unique 3D anatomic knowledge about the cerebral white matter.

Few anatomic studies have used DTI-based tractography as a complementary aid.[8,25] In contrast, few of the numerous recent publications on tractography[16] have attempted to validate their results by comparing them with fiber dissections that the authors themselves have performed. In these studies, arguments as to the actual specificity of identified structures are scant, and recognition is usually based on visual comparison to existing atlases, as well as on "*a priori* knowledge" or "well-known anatomy." None of these studies used

postmortem anatomical investigations as their background. The various articles that present DTI tractography-based protocols for reconstruction of white matter bundles and test their reproducibility [Table 1] share a common absence of *de novo* anatomical investigation, but diverge in all other aspects of their methodologies.

Combining techniques related to white matter study could improve the understanding of the complex anatomic features of structures. The revival of the fiber dissection technique and its incorporation into neuroscience education should be considered. The reestablishment of white matter fiber dissection as a standard method of study is recommended, regardless of the never-ending search for superior hardware and software resources. We can now affirm that, as advocated by Ture *et al*.,[27] the fiber dissection technique enables clearer definition and provides a keener understanding of the complex structures of the brain. This is a method that provides physicians with a true appreciation of the 3D features of the brain.

In the comparison of the fiber dissection technique and tractography-based virtual dissection, some aspects should be emphasized. Tractography may underestimate axon paths, merely showing a trace in the direction of the mean vector, or may show aberrant traces. In turn, the fiber dissection technique is also limited, mostly by the complex relationships that make up the systems of fibers, which means that revealing one system may cause the destruction of another. Crossing fibers can be hard to identify and unravel even with the aid of the operating microscope, and the boundaries between parallel bundles are often unclear. Because of the complex 3D arrangement of the internal anatomy of the brain, both techniques are only capable of revealing the macroscopic anatomy of the principal fiber bundles, being unable to accurately reveal all of the bundles present (e.g., the complex system of short fibers) or the connections along their paths. A combination of these two techniques offers reciprocal advantages. The anatomical knowledge gained by fiber dissection allowed a more criterion-based selection of ROIs and made judgment of the quality of tracts reconstructed by the diffusion tensor a more conscious process. In turn, tractography makes it possible to store the reconstructed, 3D images of the tracts and present them as the operator wishes; segmented images can be shown at the same time, using different colors, to reveal the complex relationships between the fiber systems.

While there is no 100% accurate, automatic, reproducible, and widely accessible method for tract identification and reconstruction, the tried and true fundamentals of brain anatomy as learned by means of the classic fiber dissection technique could become, paradoxically, more relevant. This approach (combination of anatomic techniques) should reduce the number of false positives, but perfect accuracy of anatomic findings is unlikely.

Although it is difficult to completely characterize the accuracy of both tractography and fiber dissection, we can measure the reproducibility of tractography. It is advocated that the reliability of quantitative measurements derived from any tractography technique should be assessed before clinical application.[6,30]

If a protocol can define feasible coordinates and offers an estimate of its own reproducibility, its use for detecting systematic differences between patients and controls becomes more relevant as a tool for clinical research. Nevertheless, there does not appear to be a consensus on including reproducibility studies when publishing cerebral tractography atlases. Moreover, differences in methodology preclude any direct comparisons between studies[6] [Table 1].

Even though FA is not the best measure for spatially distinguishing between tracts, it can be affected by many factors, and has a narrow range,[6] most studies involving DTI have focused on FA and ADC measurements, which shows the importance of assessing the reproducibility of these tract parameters in this study. In many neurological diseases, DTI has shown that these diffusion properties are altered in comparison with healthy controls.[9,15,22]

Morphological interpretation of reconstructions and of quantitative diffusion data is challenging. As Ciccarelli[5] has pointed out, the use of tractography has been restricted to specialized institutions that have the infrastructure needed to use robust and clinically applicable techniques. In the absence of a consensus between authors on the ideal tractography method, or even on a method that can be used more widely, it is reasonable that each center should undertake its own preliminary reproducibility studies. Thus, the estimated reproducibility of the protocol used in subsequent studies could be made explicit, and would take into account the specific human and technological resources available.

CONCLUSIONS

The objectives of this paper were to develop a simplified protocol based on the fiber dissection technique for reconstructing major frontal lobe tracts and to test its reproducibility. In addition to presenting the findings of our objective statistical analysis, this paper aims to encourage a revival of fiber dissection and promote further studies on the combined use of these techniques. The authors believe that the findings of classical anatomic dissection and those of MRI-based virtual dissection are visually comparable and complementary in understanding the 3D structure of the white matter of the brain.

We were able to demonstrate an appropriate level of reproducibility for most fiber tracking measurements in relation to the white matter bundles tested. Our results

show that this DTI protocol for frontal lobe tracts is suitable for clinical application, particularly for FA and ADC measurements.

REFERENCES

1. Bonekamp D, Nagae LM, Degaonkar M, Matson M, Abdalla WM, Barker PB, *et al*. Diffusion tensor imaging in children and adolescents: Reproducibility, hemispheric, and age-related differences. Neuroimage 2007;34:733-742.
2. Burgel U, Amunts K, Hoemke L, Mohlberg H, Gilsbach JM, Zilles K. White matter fiber tracts of the human brain: Three-dimensional mapping at microscopic resolution, topography and intersubject variability. Neuroimage 2006;29:1092-105.
3. Burkhalter A, Bernardo KL, Charles V. Development of local circuits in human visual cortex. J Neurosci 1993;13:1916-31.
4. Catani M, Thiebaut de Schotten M. A diffusion tensor imaging tractography atlas for virtual *in vivo* dissections. Cortex2008;44:1105-32.
5. Ciccarelli O, Catani M, Johansen-Berg H, Clark C, Thompson A. Diffusion-based tractography in neurological disorders: Concepts, applications, and future developments. Lancet Neurol 2008;7:715-27.
6. Ciccarelli O, Parker GJ, Toosy AT, Wheeler-Kingshott CA, Barker GJ, Boulby PA, *et al*. From diffusion tractography to quantitative white matter tract measures: A reproducibility study. Neuroimage 2003;18:348-59.
7. Danielian LE, Iwata NK, Thomasson DM, Floeter MK. Reliability of fiber tracking measurements in diffusion tensor imaging for longitudinal study. Neuroimage 2010;49:1572-80.
8. Fernandez-Miranda JC, Rhoton AL Jr., Alvarez-Linera J, Kakizawa Y, Choi C, de Oliveira EP. Three-dimensional microsurgical and tractographic anatomy of the white matter of the human brain. Neurosurgery 2008;62:989-1026.
9. Gupta RK, Saksena S, Hasan KM, Agarwal A, Haris M, Pandey CM, *et al*. Focal Wallerian degeneration of the corpus callosum in large middle cerebral artery stroke: Serial diffusion tensor imaging. J Magn Reson Imaging 2006;24:549-55.
10. Hagler DJ Jr, Ahmadi ME, Kuperman J, Holland D, McDonald CR, Halgren E, *et al*.Automated white-matter tractography using a probabilistic diffusion tensor atlas: Application to temporal lobe epilepsy. Hum Brain Mapp 2009;30:1535-47.
11. Holodny AI, Gor DM, Watts R, Gutin PH, Ulug AM. Diffusion-tensor MR tractography of somatotopic organization of corticospinal tracts in the internal capsule: Initial anatomic results in contradistinction to prior reports. Radiology 2005;234:649-53.
12. Hopkins HG. A new view of statistics: Effect magnitudes [Internet]. 2006 [updated 2006 Aug 7].Available from:http://www.sportsci.org/resource/stats/effectmag.html. [Last accessed on 2006 Aug 7]
13. Hua K, Zhang J, Wakana S, Jiang H, Li X, Reich DS, *et al*. Tract probability maps in stereotaxic spaces: Analyses of white matter anatomy and tract-specific quantification. Neuroimage 2008;39:336-47.
14. Huang H, Zhang J, van Zijl PC, Mori S. Analysis of noise effects on DTI-based tractography using the brute-force and multi-ROI approach. Magn Reson Med 2004;52:559-65.
15. Iwata NK, Aoki S, Okabe S, Arai N, Terao Y, Kwak S, *et al*. Evaluation of corticospinal tracts in ALS with diffusion tensor MRI and brainstem stimulation. Neurology 2008;70:528-32.
16. Jellison BJ, Field AS, Medow J, Lazar M, Salamat MS, Alexander AL. Diffusion tensor imaging of cerebral white matter: A pictorial review of physics, fiber tract anatomy, and tumor imaging patterns. AJNR Am J Neuroradiol 2004;25:356-69.
17. Johansen-Berg H, Behrens TE. Just pretty pictures? What diffusion tractography can add in clinical neuroscience. Curr Opin Neurol 2006;19:379-85.
18. Kier EL, Staib LH, Davis LM, Bronen RA. Anatomic dissection tractography: A new method for precise MR localization of white matter tracts. AJNR Am J Neuroradiol 2004;25:670-6.
19. Lawes IN, Barrick TR, Murugam V, Spierings N, Evans DR, Song M, *et al*. Atlas-based segmentation of white matter tracts of the human brain using diffusion tensor tractography and comparison with classical dissection. Neuroimage 2008;39:62-79.
20. Malykhin N, Concha L, Seres P, Beaulieu C, Coupland NJ. Diffusion tensor imaging tractography and reliability analysis for limbic and paralimbic white matter tracts. Psychiatry Res 2008;164:132-142.
21. Mandelstam SA. Challenges of the anatomy and diffusion tensor tractography of the meyer loop. AJNR Am J Neuroradiol 2012;33:1204-10.
22. Matsuo K, Mizuno T, Yamada K, Akazawa K, Kasai T, Kondo M, *et al*. Cerebral white matter damage in frontotemporal dementia assessed by diffusion tensor tractography. Neuroradiology 2008;50:605-11.
23. O'Donnell LJ, Kubicki M, Shenton ME, Dreusicke MH, Grimson WE, Westin CF. A method for clustering white matter fiber tracts. AJNR Am J Neuroradiol 2006;27:1032-6.
24. Park HJ, Kubicki M, Westin CF, Talos IF, Brun A, Peiper S, *et al*. Method for combining information from white matter fiber tracking and gray matter parcellation. AJNR Am J Neuroradiol 2004;25:1318-24.
25. Rubino PA, Rhoton AL Jr., Tong X, Oliveira E. Three-dimensional relationships of the optic radiation. Neurosurgery 2005;57:219-27.
26. Thiebaut de Schotten M, Ffytche DH, Bizzi A, Dell'Acqua F, Allin M, Walshe M, *et al*. Atlasing location, asymmetry and inter-subject variability of white matter tracts in the human brain with MR diffusion tractography. Neuroimage 2011;54:49-59.
27. Ture U, Yasargil MG, Friedman AH, Al-Mefty O. Fiber dissection technique: Lateral aspect of the brain. Neurosurgery 2000;47:417-26.
28. Van Hecke W, Leemans A, Sijbers J, Vandervliet E, Van Goethem J, Parizel PM. A tracking-based diffusion tensor imaging segmentation method for the detection of diffusion-related changes of the cervical spinal cord with aging. J Magn Reson Imaging 2008;27:978-91.
29. Verhoeven JS, Sage CA, Leemans A, Van Hecke W, Callaert D, Peeters R, *et al*. Construction of a stereotaxic DTI atlas with full diffusion tensor information for studying white matter maturation from childhood to adolescence using tractography-based segmentations. Hum Brain Mapp 2010;3:470-486.
30. Wakana S, Caprihan A, Panzenboeck MM, Fallon JH, Perry M, Gollub RL, *et al*. Reproducibility of quantitative tractography methods applied to cerebral white matter. Neuroimage 2007;36:630-44.
31. Xia Y, Turken U, Whitfield-Gabrieli SL, Gabrieli JD. Knowledge-based classification of neuronal fibers in entire brain. Med Image Comput Comput Assist Interv 2005;8(Pt 1):205-12.
32. Zhang W, Olivi A, Hertig SJ, van Zijl P, Mori S. Automated fiber tracking of human brain white matter using diffusion tensor imaging. Neuroimage 2008;42:771-7.
33. Zhang Y, Zhang J, Oishi K, Faria AV, Jiang H, Li X, *et al*. Atlas-guided tract reconstruction for automated and comprehensive examination of the white matter anatomy. Neuroimage 2010;52:1289-301.